International Communications in Heat and Mass Transfer 159 (2024) 107961

Contents lists available at ScienceDirect

International Communications in Heat and Mass Transfer

journal homepage: www.elsevier.com/locate/ichmt

New dimensionless equation for mass transfer at acetone evaporation under forced convection

Tibor Poós *, Evelin Varju

Department of Building Services and Process Engineering, Faculty of Mechanical Engineering, Budapest University of Technology and Economics, Bertalan Lajos street 4-6., H-1111 Budapest, Hungary

ARTICLE INFO

Keywords:
Evaporation rate
Acetone
Mass transfer coefficient
Volatile liquid

ABSTRACT

Equations of evaporation rate were collected from literature for different liquids. These relationships directly result in the evaporation rate or the Sherwood number. Experiments were made for vaporization of acetone from a heated vessel, at different air velocities and temperatures of air and liquid surface. The effect of the different setting parameters, and the different directions of the heat flow on the evaporation rate were studied. As expected, when the air velocity and the temperature of the liquid were higher, the evaporation was faster, but when the temperature of the air was higher, the evaporation rate was lower. Based on the measurement results, a new dimensionless equation was created to determine the evaporation rate of acetone. The new equation and the correlations from the literature were compared with the results determined from the measurement data. Two of the ten correlations did not prove to be applicable to the measurement results, three correlations showed serious deviations, while five correlations gave fairly good results. Among these five correlations, the new dimensionless equation proved to be the most accurate for determining the evaporation rate of acetone in the examined range.

1. Introduction

If gas flows over the liquid surface, between the two phases in the concentration boundary layer diffusion occurs, which is determined by the concentration gradient and the mass transfer coefficient. In this case, the gas does not diffuse into the liquid, but vapor diffuses into the gas from the surface of the liquid, which is called evaporation. Thus, the gas close to the liquid becomes saturated with vapor of the liquid while the humidity is nearly constant in the rest of the gas. If there is no air movement, a natural convection is evolved when the saturated air near to the surface moves to-wards the lower concentration air bulk. This heat capacity is usually derived from the gas bordering the liquid, where a temperature gradient is formed by the temperature difference between the bulk of gas and liquid surface, which can be balanced through the heat of conduction that is imparted to the fluid. Thus, the saturated gas in the im-mediate vicinity of the liquid surface is displaced by convection due to the buoyancy caused by the density difference and the concentration difference.

To convert the liquid to vapor, it is necessary to obtain the heat of vaporization which can come from heat capacity of the liquid and/or warmer ambient air. This heat capacity is usually derived from the gas bordering the liquid, where a temperature gradient is formed by the temperature difference between the bulk of gas and liquid surface, which can be balanced through the heat of conduction that is imparted to the fluid.

From the directions of heat and mass transfer flows, Sartori [1] states that five cases can be distinguished. In the first two cases, the temperature difference induces the diffusion, while in the third case, when the temperature of the air and liquid is the same, the difference in humidity is the driving force. These three cases can be seen in the Fig. 1. In the fourth case there is also diffusion, but since the liquid surface temperature is lower than the dew point temperature, the moisture transfer occurs in the form of condensation. In the fifth case there is no mass transfer as the air and liquid temperatures are the same, and there is no partial pressure difference between the air and the surface of the liquid, they are in equilibrium.

Most of the articles in the literature deal with the evaporation of water at natural ($v_G < 0.12\ m/s$) or forced ($v_G > 0.12\ m/s$) convection [2]. For examination of forced convection, experiments were carried out under laboratory conditions [3–6] using a measuring instrument assembled for this purpose. In addition to the laboratory experiments, the researchers also dealt with evaporation of natural lakes [7–9],

* Corresponding author.
E-mail addresses: poos.tibor@gpk.bme.hu (T. Poós), varju.evelin@gpk.bme.hu (E. Varju).

https://doi.org/10.1016/j.icheatmasstransfer.2024.107961

Available online 24 August 2024

indoor and outdoor swimming pools [10–12], cooling ponds [13], and solar ponds [14,15].

In 1802, Dalton pioneered the description of evaporation through empirical hydrodynamic approximation. Subsequently, numerous researchers have explored the phenomenon of liquid evaporation over the centuries, building upon Dalton's foundational work. Through regression analysis utilizing measurements, correlations have been established to effectively characterize the evaporation process. However, the equations derived from these studies exhibit validity within specific ranges of interpretation, encompassing variations in gas and liquid temperatures, as well as surface area and they are operating under specific conditions like natural or forced convection. This contextual limitation diminishes their practical applicability.

Most of the equations to determine the evaporation rate are based on the gas velocity and the liquid vapor partial pressure difference in the bulk gas and the liquid surface temperature:

$$N = (a + bv_G)\left(p_{v,sat,f} - p_{v,G}\right)^n \tag{1}$$

where *a, b* and *n* are constants.

There are equations, which use the relation between Sherwood, Reynolds and Schmidt numbers to describe the phenomenon:

$$Sh = aRe^b Sc^c. \tag{2}$$

where the dimensionless *Sh* number can be calculated as follow:

$$Sh = \frac{k_c L}{D_{LG}}, \tag{3}$$

the *Re* number can be determined:

$$Re = \frac{v_G L}{\nu_G}, \tag{4}$$

and the *Sc* number can be calculated by this equation:

$$Sc = \frac{\nu_G}{D_{LG}}. \tag{5}$$

There are very few articles in the literature dealing with the evaporation of volatile liquids with an open surface, and there are even fewer studies that include a correlation for determining the evaporation rate of a given volatile liquid. Table 1 shows the equations that can be used to determine the evaporation rate of volatile liquids. In addition to the equation suitable for calculating the evaporation rate, the table contains the parameters for which the equation is valid: the temperature (T_G), relative humidity (φ) and velocity of the flowing air above the liquid surface; surface temperature (T_f) of the liquid; partial pressure of the air in the bulk air $(p_{v,G})$ and above the liquid surface $\left(p_{v,f}\right)$; the vapor pressure difference between the bulk air and the liquid surface (Δp_v); the size (A_{evap}) and the shape of the liquid surface.

Bennett and Meyers [16] theoretically derived their equation for mass transfer for the case of a flat plate based on the analogy of heat transfer. Raj and Morris [17] developed an evaporation model for non-cryogenic liquids, in which convective heat transfer by the wind, convective heat transfer from the environment and the soil, and the solar radiation were taken into account. The established correlation was compared with experimental results for the evaporation of liquid dinitrogen tetroxide. Braun and Caplan [18] investigated the evaporation rate of 15different organic liquids, during which they created a relationship in which only molar mass, air velocity and partial pressure difference are included. Their measurements were made in a narrow air channel, where evaporation from a shallow 140 × 140 × 25mm tank was investigated. A total of 150 measurements were performed at three different air velocities and air temperatures.

During the measurements, the liquid level was kept at a constant value with the help of a liquid replacement container. The evaporation rate was traced back to mass measurement by measuring the mass of this outer container. Hummel et al. [20] used the same experimental results to create their own correlation, which was already a much more complicated and complex expression than in the case of Braun and Caplan.

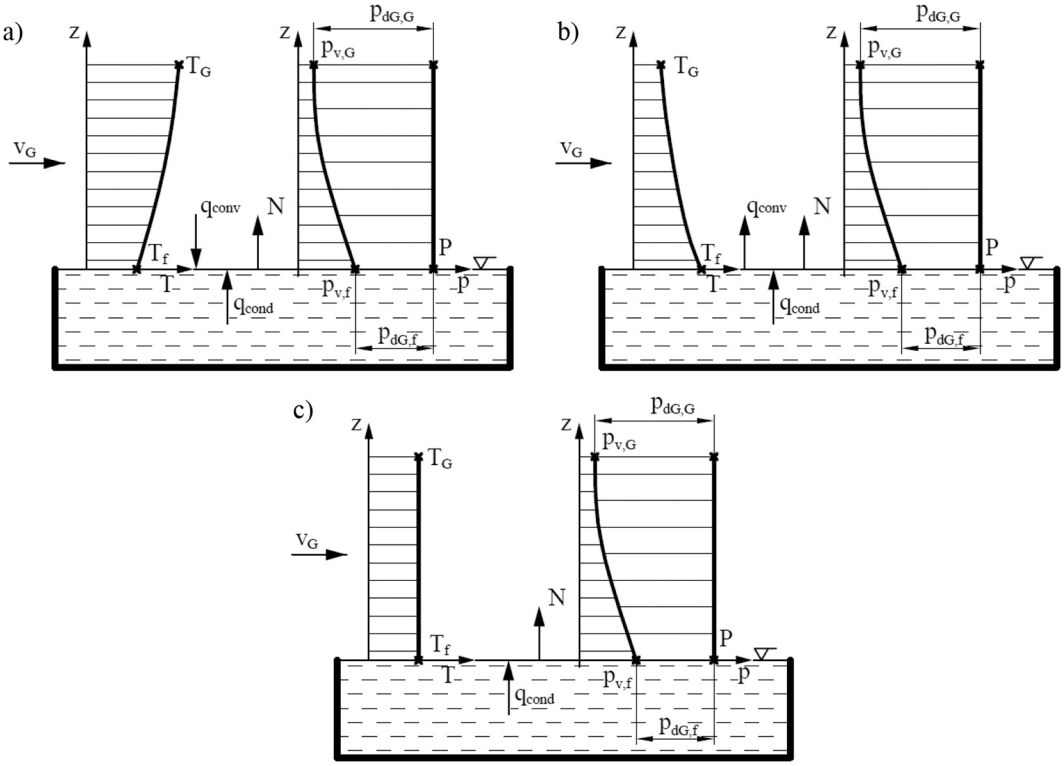

Fig. 1. Partial pressure difference and temperature-based driving forces at the five cases of liquid evaporation.

Table 1
Correlations of evaporation rate for volatile liquids and the measurement conditions.

Ref.	Authors	Equation in SI	Eq. No.	Measurement conditions										Liquid type
				T_f	v_G	T_G	φ	$p_{v,f}$	$p_{v,G}$	Δp_v	L	A_{evap}	*Shape*	
				[°C]	[m/s]	[°C]	[1]	[kPa]	[kPa]	[kPa]	[m]	[m^2]		
[16]	Bennett and Meyers	$Sh = 0.664 Re^{0.5} Sc^{1/3}$	(6)	–	–	–	–	–	–	–	–	–	–	theoretical correlation
[17]	Raj and Morris	$Sh = 0.037\left(Re^{0.8} - 15500\right) Sc^{1/3}$	(7)	−5	–	18	–	–	–	–	1.22	1.49	□	non-cryogenic liquids
[18]	Braun and Caplan	$N = 2.577{\cdot}10^{-9} M_L \left(p_{v,sat,f} - p_{v,G}\right) v_G{}^{0.625}$	(8)	-10-45	0.5–8	5–60	–	0.002–10.8	0	–	0.14	0.02	□	15 organic liquids
[19]	Olander	$N = 2.25{\cdot}10^{-6} v_G^{0.8} A^{-0.1} (T_G + 273.15)^{-0.8} M_L p_{v,sat,f} \left[\frac{\left(3.1 + \left(\frac{1000\rho_L}{M_L}\right)^{-1/3}\right)^2}{(T_G + 273.15)^{0.5} \left(\frac{1}{29} + \frac{1}{M_L}\right)^{0.5}} \right]^{-2/3}$	(9)	–	–	–	–	–	–	–	–	–	○	–
[20]	Hummel et al.	$N = 3.123{\cdot}10^{-5} M_L p_{v,sat,f} \left(\frac{1}{M_L} + \frac{1}{M_G}\right)^{0.25} \frac{1}{(T_f + 273.15)^{0.05}} \sqrt{\frac{v_G}{LP/101325}}$	(10)	-10-45	0.5–8	5–60	–	0.002–11.8	0–1.2	–	0.14	0.02	□	15 organic liquids
[21]	US EPA	$N = \frac{1.756{\cdot}10^{-5} v_G{}^{0.78} M_L{}^{2/3} p_{v,sat,f}}{R(T_G + 273.15)}$	(11)	25–50	–	–	–	–	–	–	–	–	–	toxic liquids
[22]	ERG	$N = \frac{4.503{\cdot}10^{-6} v_G{}^{0.78} \left(\frac{18}{M_L}\right)^{1/3} M_L p_{v,sat,f}}{R\left((T_G + 273.15)\frac{9}{5}\right)}$	(12)	–	–	–	–	–	–	–	–	–	–	VOCs from paint and ink
[23]	Heymes et al.	$Sh = 0.145 Re^{0.69} Sc^{0.87}$	(13)	-2-23	1.6–4	33–36	–	–	–	–	0.228	0.0433	▭	2-propanol, 1-hexene, propionaldehyde, acetone, water
[24]	Varju and Poós	$Sh = 0.24 Ri^{0.03} Re^{0.7} Sc^{1/3} \Phi_T{}^{-2} \Phi_P{}^{0.1}$	(14)	1–61	0.17–5.7	-19-79	0.04–0.99			0.025–10	0.12–1.04	0.015–1.09	–	water

Heymes et al. [23] determined a correlation between Sherwood, Schmidt and Reynolds number based on their own measurements. The measurements were carried out on a laboratory measuring device for volatile organic compounds (2-propanol, 1-hexene, propionaldehyde, acetone) and water. In the first series of measurements, the evaporation of the five materials was examined at the same time at a given ambient temperature and air velocity. While in the second series of measurements, the evaporation of acetone was investigated as a function of the effect of air velocity. Their obtained equation was validated by measuring the evaporation of ethanol, which showed a good agreement with the previously determined relationship. Varju and Poós [24] investigated evaporation under natural, mixed and forced convection for the case of water. They carried out their own measurements on a laboratory measuring device. They used their own measurement results and the results of other researchers found in the literature to create a dimensionless equation to describe liquid evaporation under natural, mixed and forced convection. Their relationship includes the *Ri* number, which can be determined using the following equation:

$$Ri = \frac{Gr}{Re^2} = \left(\rho_{G,G} - \rho_{G,f}\right) \frac{Lg}{v_G{}^2 \overline{\rho}_G}. \tag{6}$$

The temperature correction term in the equation can be calculated as follows:

$$\Phi_T = \frac{T_G + 273.15}{T_f + 273.15}, \tag{7}$$

and the correlation of the pressure correction term:

$$\Phi_p = \frac{\Delta p_v}{P}. \tag{8}$$

The studies of Olander [19] were part of several further researches, because in his work he collected the physical and chemical properties of air and air pollutants in the framework of a literature review. Tugyi et al. [25] also investigated the evaporation of acetone at four different air velocities. The measuring device consisted of a narrow air channel and a shallow vessel with a surface area of 0.00096 m^2. The vessel was placed on a scale, so the evaporation rate was converted back to a mass measurement. A report issued by the United States Environmental Protection Agency (US EPA) primarily provides guidance for a statutory risk management program [21]. Its purpose was to assist facilities working with hazardous chemicals to prevent accidental releases or mitigate the consequences. The equation in Table 1 determines the evaporation rate of liquid from a container with an open surface. The report published by the Eastern Research Group (ERG) mainly presents the methods, procedures and correlations suitable for determining the various gas and liquid emissions in the case of paint and ink plants [22]. The equation in the table describes the evaporation of volatile components onto paint or ink from an open container.

During our research, we examined the evaporation rate of acetone using an experimental measuring device. Acetone was vaporized at different air temperatures, liquid temperatures, and air velocities. We determined the value of the evaporation rate from the measurements and compared it with the values calculated from the correlations found in the literature and the new dimensionless equation.

2. Experimental material, apparatus and methods

During our investigations, we evaporated acetone as a volatile liquid in a laboratory measuring equipment built to test evaporation. The main operating parameters affecting evaporation (air and liquid temperature, air velocity) can be regulated at the measuring station.

2.1. Experimental material

Acetone is a volatile organic compound (VOC) and one of the oldest chemical compounds used for industrial purposes. The density of the acetone is 784 kg/m^3, its boiling point is 56.3 $^{\circ}C$ and its dynamic viscosity is 0.316 *mPas*. Acetone is used as a solvent for other cosmetic products, including makeup and skin creams [26] Acetone is also used as a solvent in the pharmaceutical industry as denaturant in denatured alcohol [27]. Due to the unstable properties of acetylene, it must be stored and transported under special conditions. Acetone is a flammable compound, but acetylene dissolved in liquid acetone, the transportation and storage can safely be solved [28]. Last but not last, acetone is used to clean electronic devices and components. Acetone is not used as a clean solvent, but as a single active ingredient of the electronic cleaners [26]. As described above, it is proven that acetone an important solvent, whose properties are essential for accurate use. Evaporation of the liquid is one of these relevant properties.

2.2. Experimental apparatus

The evaporation measurements were conducted using equipment available at the Department of Building Services and Process Engineering in Budapest University of Technology and Economics. Fig. 2 displays a visual representation of this equipment. The types and characteristics of the measuring devices and regulators placed on the measuring equipment are described in Table 2.

Air movement is facilitated by a centrifugal fan (type: NVH50) (P-101-01) powered by an EVIG electric motor (type: VZ32/2 max. rotational speed 2890 $1/min$). Beginning at the suction section, airflow is regulated using an orifice flow meter (P-101-01) installed on a 200 *mm* diameter pipe. A U-tube manometer gauges the pressure difference across the orifice flow meter. Air velocity adjustments are made possible through a frequency converter and a butterfly valve (V-101-01). Heating of the air is achieved with a 21 *kW* electric heater (type: Thermo-Team LF-36, accuracy: 0.5 $^{\circ}C$) (*H*-101-01), which offers both regulated and fixed performances of 9 + 6 *kW*. Following the fan, a diffuser section houses a flow damping element (D-102-01) to maintain laminar flow in the evaporation section (E-102-01). Within this section is the thermo vessel (type: Grant GLS Aqua 12 Plus) (T-102-01), containing the liquid subject to evaporation. The liquid temperature can be adjusted $T_L = T_{amb} - 99^{\circ}C$, with a stability of 0.1 °C. The thermo vessel has a maximum volume of 12 dm^3, with an open evaporating surface measuring 325 *mm x* 300 *mm*. Both the thermo vessel and the scales (type: Sartorius Signum 1, accuracy: 1 *g*) (S-102-01) beneath it are situated on a manually adjustable elevator (*L*-102-01). By altering the elevator height, the liquid surface within the thermo vessel can be positioned approximate to the bottom of the air tunnel. Finally, the humid gas exits the system through a chimney (F-102-01), dissipating into the ambient environment.

2.3. Experimental method

The measurement process initiates with the filling of the thermo vessel with acetone, followed by precise adjustment of the liquid temperature (TRC-102-01) through activation of the heating system. Subsequently, upon switching on the fan at a predetermined rotational speed (SIC-101-01), the desired air temperature (TIC-101-01) can be adjusted using the electric heater. Prior to commencing the measurement, the apparatus operates empty until reaching a stationary state, as indicated by stabilized values measured by the thermometers. Flow rate adjustments are facilitated by the butterfly valve (FIC-101-01), with determination based on the pressure difference (PDI-101-01) measured at the orifice flow meter. Before commencing the measurement, any evaporated acetone must be compensated for until the acetone surface aligns with the bottom of the air tunnel. At the outset of the measurement, both the temperature (TR-101-01) and humidity (XR-101-01) of the ambient air are determined. Evaporation properties are recorded using a data logger (type: Ahlborn Almemo 2590-9). The mass of evaporated acetone is measured by the scales (WR-102-01), while the

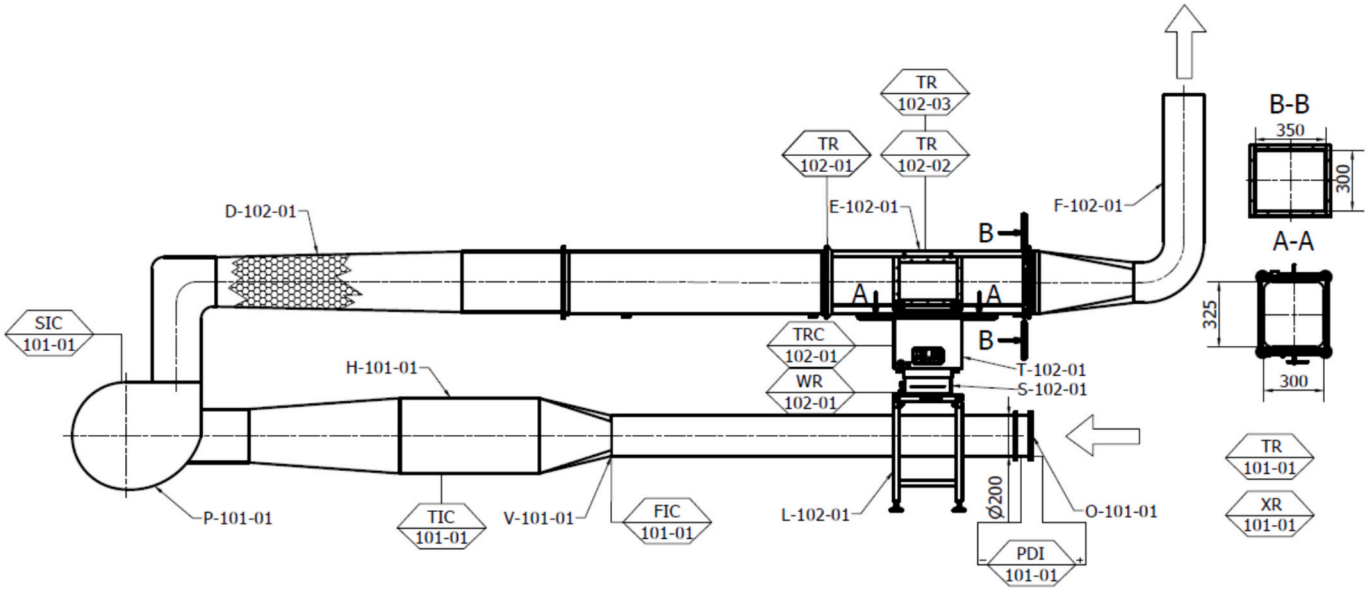

Fig. 2. Instrumented flow diagram of the measurement equipment.

Table 2
Instrumentation specification.

ID	Designation	Measured/regulated quantity	Range and accuracy
TR-101-01	ALMEMO D6 FHAD 36 Rx digital temperature and humidity meter	Ambient temperature of dry air	$-100-200\,^{\circ}C \pm 0.2\,^{\circ}C$
PR-101-01	ALMEMO D6 FHAD 36 Rx digital temperature and humidity meter	Pressure of ambient air	$700-1100\,mbar \pm 2.5\,mbar$
XR-101-01	ALMEMO D6 FHAD 36 Rx digital temperature and humidity meter	Relative humidity of ambient air	$0-100\% \pm 1.3\%$
PDI-101-01	MTA Kutesz U-tube manometer	Pressure difference measured on the orifice flow meter	$0-40\,mm \pm 0.5\,mm$
FIC-101-01	Butterfly valve	Regulate air flow rate after the heater	0–90°
TIC-101-01	JUMO ITRON 04 air heating temperature controller	Air flow temperature regulator	$T_{amb}-100\,^{\circ}C \pm 0.5\,^{\circ}C$
SIC-101-01	Schneider Electric Altivar 312 frequency converter	Regulate air flow rate after the heater	$\sim 500-2880\,1/min$
TR-102-01	T-type thermocouple	Temperature of air above the liquid surface	$-200-400\,^{\circ}C \pm 0.1\,^{\circ}C$
TR-102-02	AHLBORN AMiR 7842 infrared meter	Liquid surface temperature	$0-500\,^{\circ}C \pm 1\,^{\circ}C$
TR-102-03	T-type thermocouple	Bulk temperature of liquid	$-200-400\,^{\circ}C \pm 0.1\,^{\circ}C$
WR-102-01	Sartorius Signum 1 scale	Mass of evaporated liquid	$0-65\,kg \pm 1\,g$
TRC-102-01	Heating regulator of Grant GLS Aqua 12 Plus	Temperature of liquid	$T_{amb}-99\,^{\circ}C \pm 0.1\,^{\circ}C$

surface temperature of the acetone (TR-102-02) is recorded using an infrared thermometer (type: AMiR 7842) positioned above the thermo vessel. Additionally, the temperature of the gas (TR-102-01) and the bulk liquid (TR-102-03) is measured using a T-type thermometer. These measured values are then logged by the Apollo module of the IMPERIUM Laboratory Information System [29], with the option to set the sampling time.

2.4. Evaluation method

During the measurements of acetone evaporation, the following parameters were recorded: the temperature (T_{amb}), relative humidity (φ) and absolute pressure (P_{amb}) of ambient air; the pressure drop measured on the orifice flow meter by the U-tube manometer (Δh); the temperature of the flowing air above the liquid surface in the channel (T_G), the bulk temperature (T_L) and surface temperature (T_f) of the acetone; mass of the evaporated acetone (Δm) and elapsed time (t).

The aim of our work is to compare the *Sh* numbers determined from the Eqs.(6)–(14) with values calculated from evaporation measurements. First, the evaporation rate was determined using the measured values:

$$N_{meas} = -\frac{\Delta m}{\Delta t A}, \tag{9}$$

The evaporation rate can be written by the molar concentration difference interpreted near the surface of acetone and on the bulk of the air, where the proportionality term is the mass transfer coefficient:

$$N_{meas} = k_{c,meas} M_L \left(c_f - c_G\right). \tag{10}$$

In our case, the initial concentration of acetone vapor in the air is negligible $(c_G \approx 0)$. The equilibrium concentration in the immediate vicinity of the surface can be calculated based on the ideal gas law:

$$c_f = \frac{p_{v,sat,f}}{R\left(T_f + 273.15\right)}, \tag{11}$$

where $p_{v,sat,f}$ is the saturated vapor partial pressure at the acetone surface temperature.

By substituting Eq.(20) into Eq.(19) we obtain the mass transfer coefficient calculated from the measurement results:

$$k_{c,meas} = \frac{N_{meas} R\left(T_f + 273.15\right)}{p_{v,sat,f} M_L}. \tag{12}$$

Knowing the mass transfer coefficient, the *Sh* number can be calculated:

$$Sh_{meas} = \frac{k_{c,meas} L}{D_{LG}}, \tag{13}$$

where the characteristic size of the thermos vessel in the flow direction is $L = 0.3\,m$. The diffusion coefficient can be calculated using the following relationship for acetone-air [30,31]:

$$D_{LG} = \frac{1.498 \cdot 10^{-6} (T + 273.15)^{1.81} \left(\frac{1}{M_L} + \frac{1}{M_G}\right)^{0.5}}{\left(\frac{P}{101325}\right) \left(T_{cr,L} T_{cr,G}\right)^{0.1405} \left(V_{cr,L}^{0.4} + V_{cr,G}^{0.4}\right)^2}, \quad (14)$$

where T is the examined temperature in $^{\circ}C$; P is the athmospheric pressure in Pa; $M_L$and M_G are the molar masses of acetone and air, $M_L = 58.08\ kg/kmol$, $M_G = 28.96\ kg/kmol$; $T_{cr,L}$ and $T_{cr,G}$ are the critical temperatures of acetone and air $T_{cr,L} = 508.1\ K, T_{cr,G} = 132.4\ K$; P is the total atmospheric pressure $[Pa]$; $V_{cr,L}$ and $V_{cr,G}$ are the critical molar volumes of acetone and air $V_{cr,L} = 209\ cm^3/mol, V_{cr,G} = 93.35\ cm^3/mol$.

This correlation below $P = 5 \cdot 10^5\ Pa$ is independent of the concentration, and its average absolute deviation is 5.64 % and its standard deviation is ±7.21 %.

2.5. Statistical analysis

The Sh_{meas} values determined from the measurement results and the Sh_{calc} values determined from the correlations were compared using statistical analysis. The purpose of the study was to select an equation suitable for describing the evaporation rate of acetone in the given measurement range. For this, we determined the average relative error (RE), which shows how large the absolute error is compared to the measured value:

$$RE = \frac{1}{j} \sum_{i=1}^{j} \frac{\left|Sh_{calc,i} - Sh_{meas,i}\right|}{Sh_{calc,i}}. \quad (15)$$

The root mean square error ($RMSE$) shows the standard deviation of the data around the regression line. The smaller its value, the better the fit between the calculated and measured value, but it is sensitive to large differences:

$$RMSE = \sqrt{\frac{1}{j} \sum_{i=1}^{j} \left(Sh_{calc,i} - Sh_{meas,i}\right)^2}. \quad (16)$$

The coefficient of determination (R^2) can be used to characterize the relationship between the measured values and the values calculated from the correlation. The better the fit, the closer we are to 1, but it can also take a negative value. The indicator is sensitive to outliers. The coefficient of determination can be determined:

$$R^2 = 1 - \frac{\sum_{i=1}^{j} \left(Sh_{meas,i} - Sh_{calc,i}\right)^2}{\sum_{i=1}^{j} \left(Sh_{meas,i} - \overline{Sh_{meas}}\right)^2}. \quad (17)$$

The Bland-Altman method can be used to further investigate the relationship between the Sh number values determined by the correlations and calculated from measurement data sets. This method is suitable for analyzing the difference and the average between the Sh number values calculated from the correlations and determined from the measurement data, where the goal is to examine the similarity of the two values [32]. If the two values are the same, then the points are scattered around a horizontal line, and ideally the points are located on the abscissa. If the intercept is different from 0, then there is a constant error between the two values, and if the slope is different from 0, then a proportional error can be inferred. In addition, the agreement can also be characterized by specifying the limits of the confidence interval, the majority of the points must fall within this interval. A value of 90 % was used for the confidence limits during the study.

3. Results and discussion

In the course of our research, measurements were performed on the evaporation of acetone at different air velocities, air temperatures and liquid surface temperatures. Based on these measurement results, a dimensionless equation was created for determining the evaporation rate of acetone. We compared the results given by this equation and the correlations found in the literature with the measurement results. For comparison, statistical analysis was used to determine the correlation that most accurately represents the acetone evaporation rate under given conditions.

3.1. Measurement results

In the course of measurements, adjustments were made to the air velocity (v_G), air temperature (T_G), and acetone temperature (T_L), which consequently affecting the temperature of the liquid surface (T_f). While the temperature-based driving force (ΔT) could have been modified, the absolute humidity-based driving force (ΔY) could not have been altered based on measurements. Among the five cases of evaporation investigated during the research, the first three cases were examined. These cases differed in the direction of convective heat flow while maintaining a consistent mass flow direction.

1: $T_G > T_f; Y_f > Y_G$ (the acetone temperature is lower than the air temperature)

2: $T_G < T_f; Y_f > Y_G$ (the acetone temperature is higher than the air temperature)

3: $T_G = T_f; Y_f > Y_G$ (the air and the acetone temperature are equal)

The temperature of the acetone was adjusted to its surface temperature, from which it is possible to derive the temperature driving force between the gas and liquid that important at evaporation.

Table 3 summarizes the measured properties for each measurement at evaporation of acetone, and the values of the calculated parameters from the measured properties using the method described in Chapter 2.4. During the measurements we adjusted the magnitude of the air velocity from the very low value $(0.26\ m/s)$ to the permissible maximum $(1.7\ m/s)$. At the latter value there were no waves on the surface of the liquid, so changing the surface size and droplet drift do not have a decisive effect on the results. The air temperature between $T_G = 30 - 45^{\circ}C$, the liquid surface temperature between $T_f = 30 - 45^{\circ}C$ were controlled. In the latter case, due to the volatile properties of acetone, it was impossible to measure at a temperature of more than $45^{\circ}C$. Since the constant surface temperature reached, the intense evaporation caused the liquid level to be so low that it would have disrupted the image of the nearly parallel streams.

Fig. 3 shows the effect of various parameters on acetone evaporation, where the evaporated mass of acetone is in the function of time. It can be seen in Fig. 3/a that, as expected, the higher velocity of air resulted higher evaporation rate. At $1.7\ m/s$ air velocity, evaporation rate is about ten times higher than at $0.26\ m/s$. Fig. 3/b shows the effect of the liquid temperature at the same air velocity and acetone temperature, where increasing the acetone temperature resulted increasing evaporation rate. In Fig. 3/c, that trend can be seen, where the increase in the gas temperature causes the evaporation rate decrease. Fig. 3/d-f show results at the direction of heat flow in each case. From their comparison it can be seen that the highest evaporation rate occurs when the direction of heat flow is the same as the direction of the mass flow, namely from the liquid to the air. For example, if the liquid surface temperature is $45^{\circ}C$ and the air temperature is $35^{\circ}C$, evaporation rate is almost 1.5 times greater than in reversed situation.

The Fig. 3/d and Fig. 3/f diagrams also show the tendency for higher liquid temperature produces higher evaporation rate. Fig. 3/f shows that if there is no heat flow between the two phases, the common temperature affects the evaporation rate, which means that higher temperature results higher evaporation rate. This is possible because with the increase in acetone temperature decreases the heat of evaporation, the humidity difference driving force increases.

Completed the evaluation method described in Chapter 2.4, the measurement results can be seen in Table 3. From the measured data the

Table 3
Measured and calculated parameters from evaporation measurement of acetone and their relative errors.

	Measured values							Calculated values									
No.	v_G	T_G	Y_G	T_f	T_L	Δm	Δt	N	$\frac{\delta N}{N}$	k_c	$\frac{\delta k_c}{k_c}$	Sh_{meas}	$\frac{\delta Sh_{meas}}{Sh_{meas}}$	Re	$\frac{\delta Re}{Re}$	Sc	$\frac{\delta Sc}{Sc}$
	$[m/s]$	$[^\circ C]$	$[g/kg]$	$[^\circ C]$	$[^\circ C]$	$[kg]$	$[s]$	$[kg/m^2h]$	[%]	$[m/s]$	[%]	[1]	[%]	[1]	[%]	[1]	[%]
1		30.1	8.7	30.2	31.0	0.208	2538	3.03	1.18	0.00096	6.04	27.7	4.74	4880	12.51	1.55	0.25
2		30.0	10.7	35.1	37.0	0.284	2506	4.18	1.07	0.00110	5.79	31.4	4.56	4796	12.50	1.55	0.25
3		30.1	10.2	40.1	43.3	0.418	2160	7.15	0.99	0.00158	5.57	44.3	4.39	4739	12.49	1.55	0.25
4		35.0	9.5	30.4	30.1	0.331	3250	3.76	1.03	0.00118	6.00	33.6	4.71	4879	12.51	1.55	0.25
5	**0.26**	35.0	11.5	35.0	35.6	0.413	2961	5.15	0.99	0.00136	5.78	38.3	4.55	4811	12.50	1.55	0.25
6		35.0	14.9	40.1	42.5	0.497	2761	6.65	0.97	0.00147	5.56	40.5	4.38	4710	12.50	1.55	0.25
7		35.2	11.7	45.3	48.7	0.512	1770	10.68	0.97	0.00197	5.35	53.7	4.23	4653	12.48	1.55	0.25
8		40.1	12.0	18.6	14.1	0.146	2152	2.51	1.40	0.00126	6.66	36.5	5.19	5004	12.54	1.55	0.25
9		40.0	14.7	40.1	41.5	0.387	2581	5.53	1.00	0.00122	5.57	33.3	4.38	4742	12.49	1.54	0.25
10		45.1	12.0	35.1	33.2	0.483	3414	5.22	0.97	0.00138	5.78	37.6	4.53	4789	12.51	1.55	0.25
11		45.1	12.4	40.1	39.3	0.280	1648	6.27	1.07	0.00138	5.58	37.2	4.39	4719	12.50	1.55	0.25
12		30.0	8.8	30.2	31.0	0.677	1900	13.15	0.95	0.00416	6.00	120.2	4.71	10,907	2.58	1.55	0.25
13		30.0	11.4	35.0	36.9	0.682	1495	16.84	0.95	0.00446	5.78	126.9	4.55	10,710	2.58	1.55	0.25
14		30.1	10.5	40.2	43.2	0.686	1161	21.80	0.95	0.00479	5.56	134.4	4.38	10,587	2.58	1.55	0.25
15		35.0	11.2	30.1	29.6	0.523	1796	10.75	0.96	0.00341	6.00	97.2	4.71	10,949	2.58	1.55	0.25
16		35.0	11.7	35.1	35.8	0.619	1405	16.25	0.95	0.00429	5.78	120.4	4.54	10,742	2.58	1.55	0.25
17	**0.6**	35.0	15.0	40.1	42.5	0.754	1430	19.47	0.94	0.00429	5.56	118.5	4.38	10,541	2.58	1.55	0.25
18		35.1	11.6	45.4	48.8	0.573	702	30.14	0.98	0.00554	5.35	150.8	4.22	10,394	2.57	1.55	0.25
19		37.6	15.3	37.5	38.7	0.783	1647	17.54	0.94	0.00424	5.67	117.2	4.46	10,642	2.58	1.55	0.25
20		39.9	11.9	17.0	12.7	0.210	1795	4.32	1.18	0.00232	6.71	67.6	5.22	11,250	2.59	1.55	0.25
20		39.9	14.9	40.2	41.5	0.597	1159	19.02	0.96	0.00418	5.56	113.9	4.37	10,585	2.58	1.54	0.25
22		44.9	12.1	35.1	33.2	0.513	1467	12.90	0.97	0.00341	5.78	92.9	4.53	10,693	2.58	1.55	0.25
23		45.0	12.6	40.0	39.2	0.491	1105	16.39	0.98	0.00363	5.57	97.4	4.38	10,557	2.58	1.55	0.25
24		30.8	11.4	35.1	37.2	0.624	671	34.31	0.97	0.00906	5.78	257.2	4.55	20,026	0.96	1.55	0.25
25		30.0	9.1	29.7	30.4	0.799	1247	23.64	0.94	0.00763	6.02	220.7	4.73	20,430	0.96	1.55	0.25
26		34.0	15.0	37.8	40.2	0.560	536	38.58	1.00	0.00922	5.66	257.4	4.46	19,841	0.96	1.55	0.25
27		35.1	12.1	30.1	29.6	0.703	1282	20.23	0.95	0.00643	6.00	183.1	4.71	20,486	0.96	1.55	0.25
28	**1.1**	34.9	11.7	34.9	35.6	0.754	976	28.51	0.95	0.00759	5.78	213.0	4.55	20,085	0.96	1.55	0.25
29		35.0	15.0	39.3	41.7	0.590	540	40.31	0.99	0.00915	5.60	253.5	4.41	19,779	0.96	1.55	0.25
30		37.4	15.1	37.6	38.8	0.531	595	32.95	0.99	0.00795	5.67	219.9	4.46	19,892	0.96	1.55	0.25
31		40.1	15.1	40.0	41.2	0.423	390	40.05	1.06	0.00886	5.58	241.5	4.39	19,790	0.96	1.55	0.25
32		45.1	12.2	34.8	32.7	0.753	1140	24.37	0.95	0.00651	5.79	177.4	4.54	20,002	0.96	1.55	0.25
33		45.0	12.6	40.2	39.8	0.938	871	39.74	0.95	0.00872	5.55	234.2	4.37	19,750	0.96	1.55	0.25
34		30.9	9.1	29.8	30.8	0.819	794	38.09	0.95	0.01223	6.02	352.7	4.72	31,643	0.71	1.55	0.25
35	**1.7**	35.2	11.7	29.9	29.6	0.907	935	35.80	0.94	0.01145	6.01	326.0	4.71	31,618	0.71	1.55	0.25
36		45.1	12.4	34.8	33.3	0.971	897	39.97	0.94	0.01067	5.79	290.7	4.54	30,967	0.71	1.54	0.25

evaporation rate (N), the mass transfer coefficient (k_c), the Sh number, the Re number and the Sc number were obtained. The relative errors of these calculated parameters were determined based on the measurement accuracy of the instruments. It can be seen that the evaporation rate had a maximum relative error of $\delta N/N = 1.4\%$, the mass transfer coefficient $\delta k_c/k_c = 6.71\%$, the Sh number $\delta Sh/Sh = 5.22\%$, and the Sc number $\delta Sc/Sc = 0.25\%$. A higher relative error value of $\delta Re/Re \sim 12\%$ can be observed only in the case of the Re number at 0.26 m/s air velocity. This results from the reading accuracy of the U-tube manometer, which already resulted in a significant error at such a low air velocity.

In order to see the consequences of varying the different parameters on the evaporation rate, an impact examination was performed, the results can be seen in Fig. 4. The effect of ±5 °C temperature difference was tested for the evaporation rate. It has been found that evaporation of acetone increases, if the temperature of liquid and air velocity increases, and if the air temperature decreases. Although the difference is not the same for each parameter, it can be seen that the air velocity influences the most the evaporation rate. It is also observed that the temperature of the liquid has a greater influence on the evaporation rate than the temperature of the gas.

3.2. Determination of dimensionless equation

Table 3 shows the values of the dimensionless numbers calculated from the measurement data. Knowing the Sh_{meas} number, the Re number and the Sc number, the equation in the form of Eq.(2) can be established. The coefficient (a) and exponents (b, c) in Eq.(2) can be determined from the measurement results using regression analysis to describe acetone evaporation. MathWorks MATLAB software was used for the regression analysis. When optimizing the value of parameters a, b, c in the dimensionless equation, the objective function was the minimization of the relative deviations between the Sh numbers calculated from the measurement data (Sh_{meas}) and the Sh numbers calculated from the equation (Sh_{calc}). During the optimization, the tested ranges of the parameters were chosen based on literature recommendations and preliminary optimum searches. The final form of the dimensionless equation for acetone evaporation:

$$Sh = 0.002 Re^{1.16} Sc^{1/3}. \tag{18}$$

in the following validity range and measurement conditions:

$$4660 \leq Re \leq 31640$$

$$1.54 \leq Sc \leq 1.55$$

$$30^\circ C \leq T_G \leq 45^\circ C$$

$$0.25\ m/s \leq v_G \leq 1.7\ m/s$$

$$17^\circ C \leq T_f < 45^\circ C$$

Validity ranges give the limits of the intervals covered by the analysed data series. The average relative error of the equation is 15.6 %.

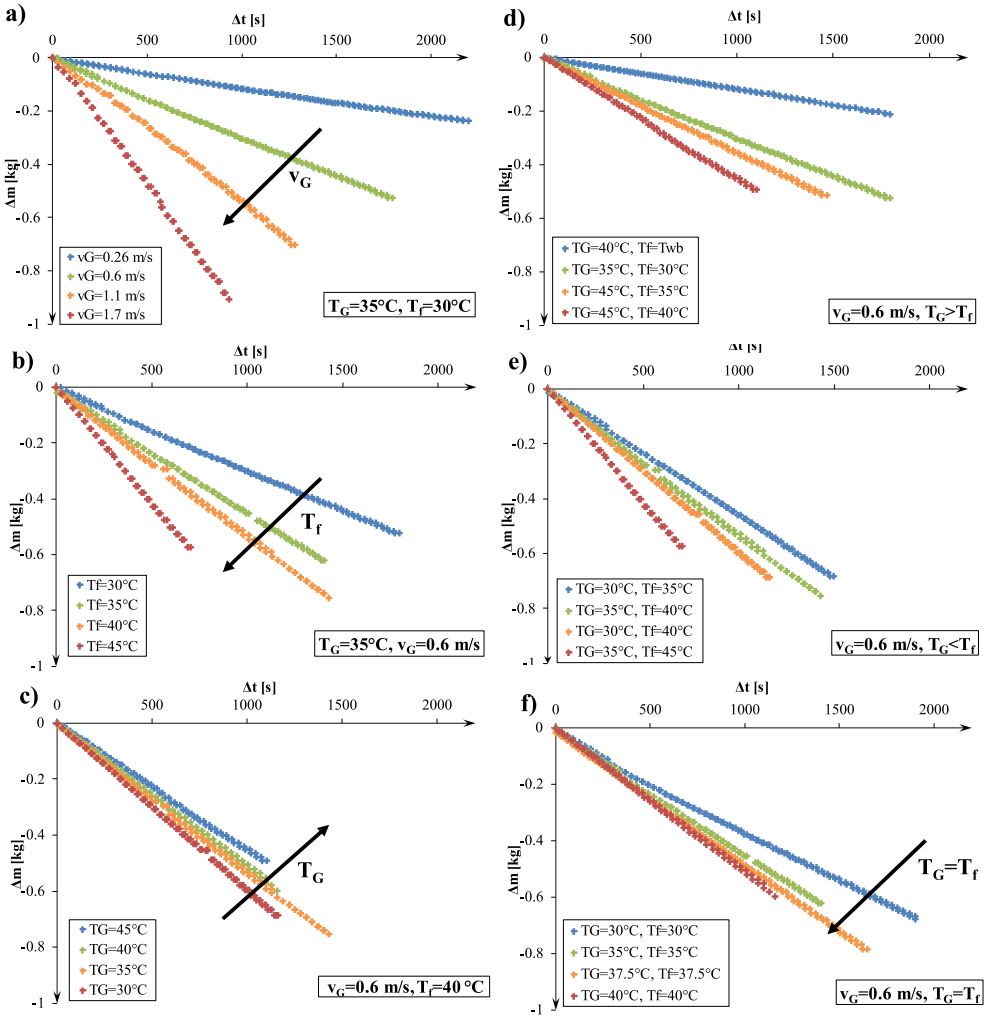

Fig. 3. Evaporated mass of acetone in the function of time a) Effect of air velocity, b) Effect of liquid temperature, c) Effect of air temperature, d)-f) Effect of convective heat flow direction.

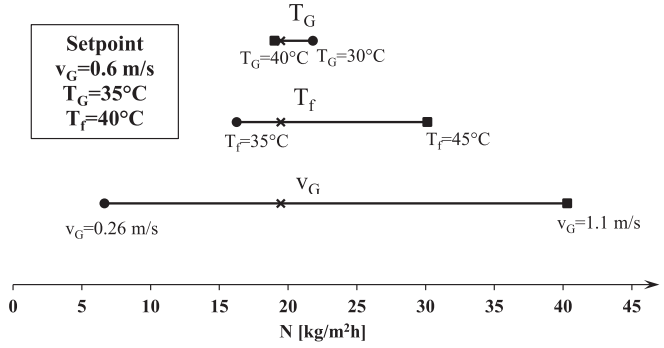

Fig. 4. Impact examination of acetone evaporation rate.

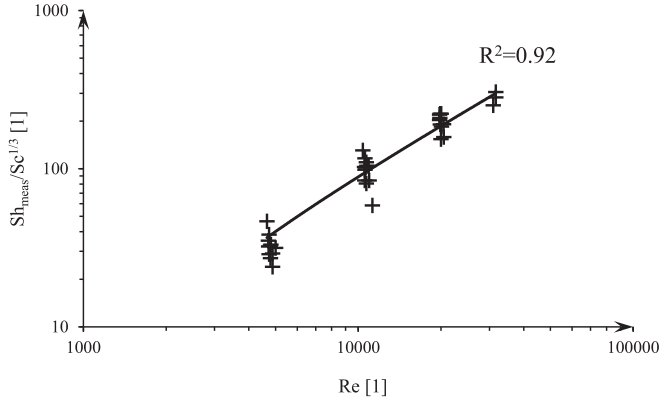

Fig. 5. The Sh_{meas} number calculated from the measurement results as a function of the *Re* number

Fig. 5 shows the Sh_{meas}–*Re* function relationship on logarithmic axes. As expected, the Sh_{meas} number value was higher in the case of a higher *Re* number. For a given *Re* number, the measurement points are located almost vertically on the diagram, depending on how the temperature values developed during the measurements.

3.3. Comparison of the equations

To obtain the Sh_{calc} value from the evaporation rate equations, there are two possibilities. For equations where the *Sh* number can be calculated directly [16,17,23,24], this can be done by defining the necessary dimensionless numbers.

However, for those equations that give evaporation rate (N_{calc}) [18–22], additional calculations must be performed there. That is, the value of the calculated mass transfer coefficient (k_{calc}) can be obtained using the equation Eq.(21) and then, using the equation Eq.(22) the value of Sh_{calc} can be determined.

Table 4
Results of the statistical analysis for acetone evaporation.

Ref.	Correlation	*RE* [1]	R^2 [1]	*RMSE* [1]
[16]	Bennett and Meyers	0.66	0.12	87.25
[18]	Braun and Caplan	0.29	0.81	40.86
[20]	Hummel et al.	0.34	0.68	52.67
[21]	US EPA	0.42	0.50	65.64
[22]	ERG	2.49	−0.90	128.50
[23]	Heymes et al.	0.27	0.84	37.34
[24]	Varju and Poós	0.30	0.79	43.11
	Eq.(27)	0.16	0.92	27.49

Chapter 1 describes the literature equations that are suitable for calculating the evaporation rate of acetone. Using the measurement data, the evaporation rates and the Sh_{calc} numbers were also determined with the help of Eqs.(6)–(14) and Eq.(27). During the evaluation, the correlations of Raj and Morris [17] and Olander [19] gave values that were so different from the measurement results that we did not examine their correlations further. The Raj and Morris equation would probably have been used at higher air velocities. Since the value of $Re^{0.8}$ did not exceed 15 500 in the measurements, the Sh_{calc} numbers calculated from their equation took a negative value. Olander's equation gave the value of the evaporation rate with deviations of orders of magnitude.

After the Sh_{calc} numbers have been determined with the evaporation rate correlations, the statistical indicators described in the Chapter 2.5 were calculated from the measurement results and the results of the equations. The result of this can be seen in Table 4.

Based on the values of the various statistical indicators, a clear order can be established for the investigated correlations and the indicators give consistent results. The worst result was given by the equation from the report prepared by the Eastern Research Group (ERG) [22]. So much so that the value of *RE* and *RMSE* is multiple of the others, and the value of R^2 became negative. The equation greatly underestimates the value of the evaporation rate over the entire investigated range. The correlation of Bennett and Meyers [16] gave better results, but still the R^2 is value very low and the *RE* and *RMSE* values are high. Their equation slightly overestimates the evaporation rate in the case of lower air velocities ($v_G < 0.5\,m/s$), while it underestimates the evaporation rate in the case of higher air velocities ($v_G < 0.5\,m/s$). The correlation in the report prepared by the US EPA [21] gave better results than these, but the higher the air velocity, the more it underestimated the value of the evaporation rate. The values of the statistical indicators for the correlation of Hummel et al. [20] were the most unfavorable from the other examined equations. Their equation gave similar results to the equation of Bennett and Meyers, overestimating the evaporation rate at low air velocities, while underestimating it at higher air velocities.

The other four correlations gave better results. No significant difference can be observed between equation of Varju and Poós [24] and the equation of Braun and Caplan [18]. The result was reported by the correlation of Heymes et al. [23] were noticeably better, but the results from the Eq.(27) was definitely the best. The values of *RE* and *RMSE* are clearly the lowest, while the value of R^2 is the highest. We examined these four correlations separately and in detail.

Fig. 6 shows the Sh_{calc} numbers determined from the correlations as a function of the Sh_{meas} number determined from the measurement in the case of the four best correlations. In general, the equations overestimated the evaporation rate at low air velocities and underestimated it at very high air velocities. Only in the results given by Eq.(27) can it be observed that, in the case of low air velocities, it returns the value of the evaporation rate more accurately, but in the case of high air velocities, it overestimates it.

In the case of the correlation by Braun and Caplan [18], Heymes et al. [23] and the Eq.(27) the four investigated air velocity values can be clearly distinguished on the diagram: the points are scattered in four horizontal bands relative to each other. While in the case of the equation by Varju and Poós [24], such a feature cannot be observed, the measurement points were evenly scattered around the line representing the

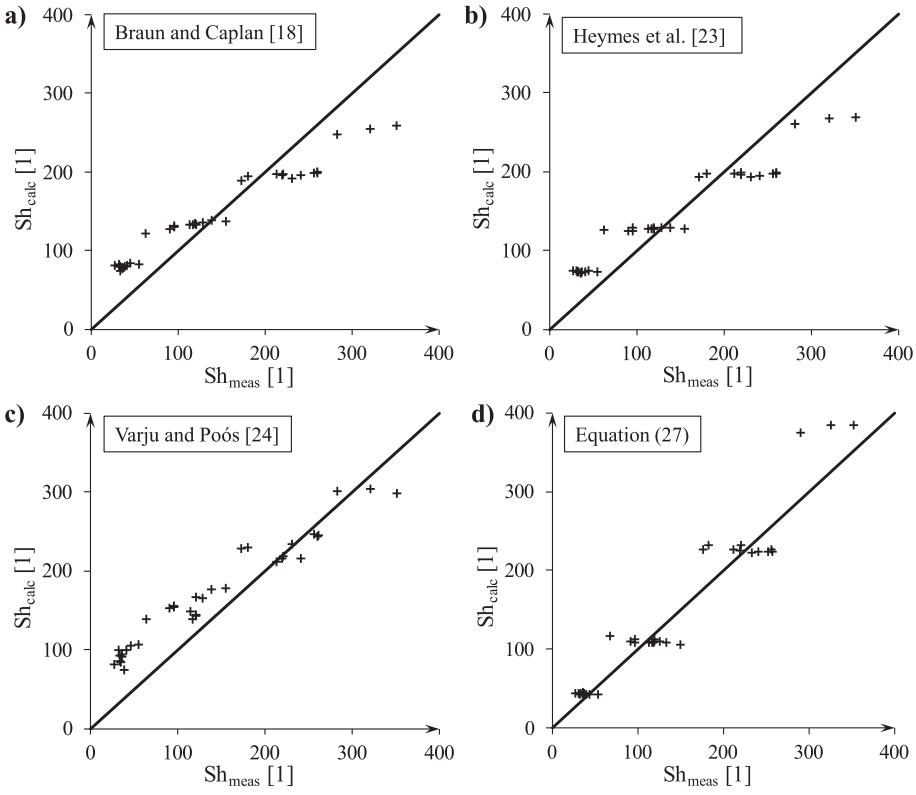

Fig. 6. Comparison of the calculated and measured *Sh* numbers for the literature equations.

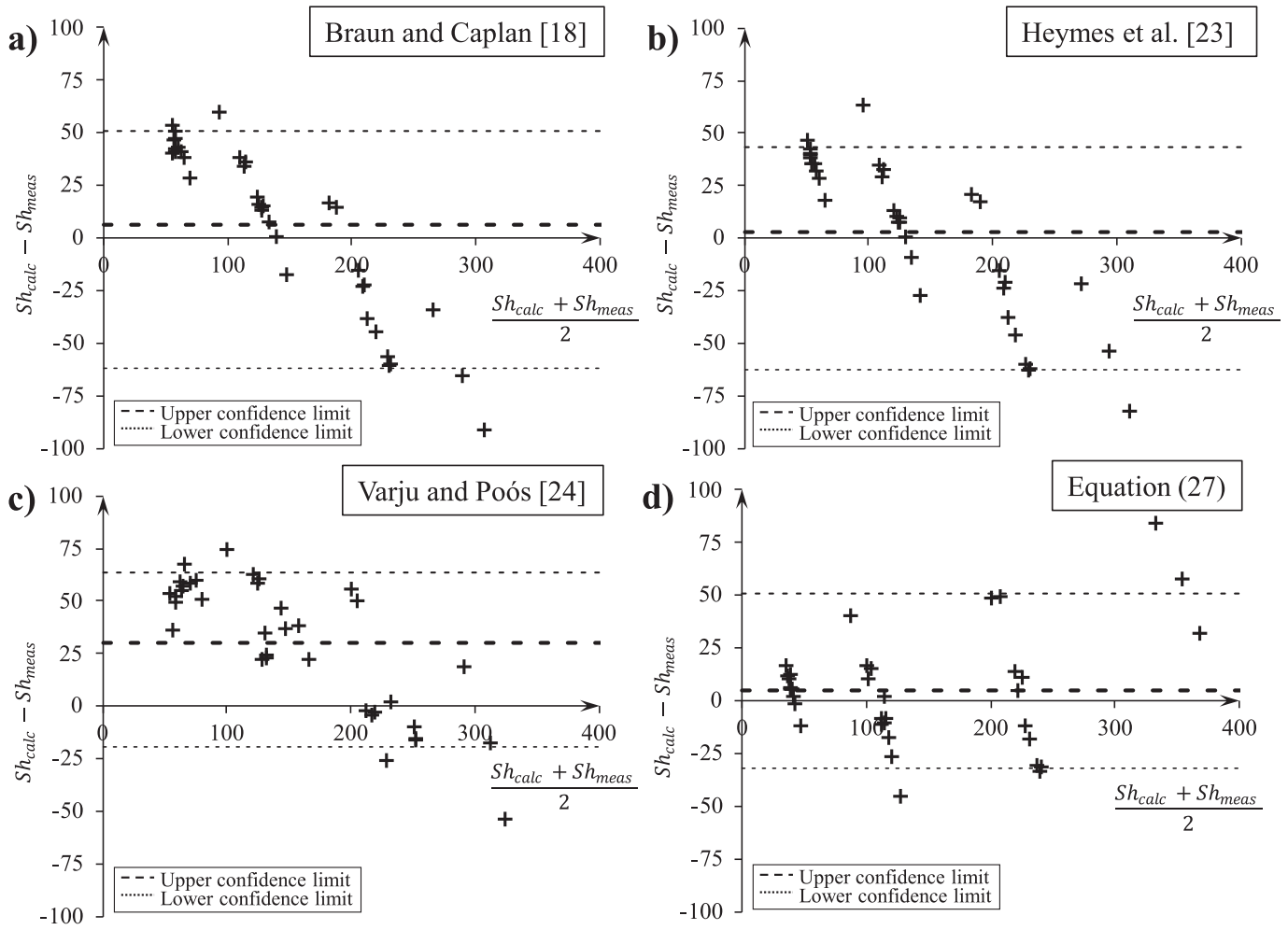

Fig. 7. The results of Bland-Altman method for the literature equations.

perfect fit.

Fig. 7 shows the results of the Bland-Altman method for the four best correlations. The diagrams show the average of the calculated and measured *Sh* number in the function of the difference between the two values. In addition, the 90 % confidence interval limits and the average of the calculated and measured *Sh* numbers can be seen. In an ideal case, the calculated values are located on the abscissa or spread around it, but in neither case is this tendency visible. For three equations [18,23,24], a proportional error can be inferred, since the slope of the line formed by the calculated values is not zero. The results of Eq.(27) show a proportional error only for larger *Sh* numbers. In the case of the equations of Varju and Poós [24], a constant distortion is also present since the axis section is quite different from zero.

The size of the confidence interval range, as well as the difference between the average of the calculated and measured *Sh* numbers, can be seen in Table 5. The smallest confidence interval can be observed in the case of the Eq.(27) and the equation of Varju and Poós [24], but the smallest axis intercept value was found by the correlation of Heymes et al. [23]. Interestingly, the correlation of Braun and Caplan [18] also gave a low value of the axis section.

Based on the Bland-Altman method and the statistical analysis, it can be said that Eq.(27) is the most suitable for determining the acetone evaporation rate in the investigated range.

Table 5
Results of the Bland-Altman method for empirical correlations for acetone evaporation.

Ref.	Correlation	Confidence interval	$\overline{Sh}_{calc} - \overline{Sh}_{exp}$
[18]	Braun and Caplan	113.2	6.2
[23]	Heymes et al.	105.6	3.1
[24]	Varju and Poós	83.2	30.0
	Eq.(27)	83.0	5.2

4. Conclusion

During our research, we investigated the evaporation of acetone under forced convection. Most of the research in the literature examined the evaporation of water, and only a small proportion dealt with the evaporation of other liquids. During the literature research, we collected publications dealing with the evaporation of various volatile liquids in the case of forced convection. During our work, we vaporized acetone at different air and liquid temperatures and air velocities. We have studied the effect of the different setting parameters, and the different directions of the heat flow on the evaporation rate. As expected, when the air velocity and the temperature of the liquid were higher, the evaporation was faster. But when the temperature of the air was higher, the evaporation rate was lower. An impact examination was performed to find out which parameters have an influence on the evaporation rate. It was found that in the case of acetone evaporation, the air velocity mostly affects the evaporation rate, and that the temperature of the liquid has a greater influence on the evaporation than the change in the temperature of the gas.

From the measurement results, we determined the value of the

evaporation rate and the *Sh* number. Using the measurement results, a new dimensionless equation was created for determining the evaporation rate of acetone. The results given by the new dimensionless equation and the correlations found in the literature were compared with the values obtained from the measurement results. The results determined from the correlations were evaluated using statistical analysis, during which various statistical indicators were determined. Among the correlations, four equations (Braun and Caplan [18], Heymes et al. [23], Varju and Poós [24] and Eq.(27)) gave good results for the evaporation rate. However, the results obtained by the new dimensionless equation Eq.(27) were the closest to the values determined from the measurement in the examined range. In the case of the Eq.(27): $RE = 0.16$, $R^2 = 0.92$, and $RMSE = 27.5$. In addition, the results were checked with the Bland-Altman method, which confirmed the previous statements.

Nomenclature

A	surface $[m^2]$
c	molar concentration $[mol/m^3]$
D	diffusion coefficient $[m^2/s]$
g	gravitational acceleration $[m/s^2]$
Gr	Grashof number for mass transfer [1]
h	difference in U-tube manometer $[m]$
k	mass transfer coefficient $[m/s]$
L	characteristic length $[m]$
m	mass $[kg]$
M	molar mass $[kg/kmol]$
N	evaporation rate $[kg/(m^2 s)]$
p	partial pressure $[Pa]$
P	total pressure $[Pa]$
q	heat flux density $[W/m^2]$
R	ideal gas constant $[8.314\ J/(mol^{\circ}C)]$
R^2	coefficient of determination [1]
$RMSE$	root mean square error [1]
RE	averaged relative error [1]
Re	Reynolds number [1]
Ri	Richardson number [1]
Sh	Sherwood number [1]
Sc	Schmidt number [1]
t	time $[s]$
T	temperature $[^{\circ}C]$
T_{cr}	critical temperature $[K]$
v	velocity $[m/s]$
V_{cr}	critical molecular volume $[cm^3/mol]$
Y	absolute humidity of gas $[kg_{moisture}/kg_{dry\ gas}]$
z	distance from the liquid surface $[m]$

Greek letters

δ	absolute error of a calculated parameter
ρ	density $[kg/m^3]$
ν	kinematic viscosity $[m^2/s]$
φ	relative humidity [1]
Φ_T	temperature correction term [1]
Φ_p	vapor pressure correction term [1]

Subscripts and superscripts

a, b, c, n	superscripts in Eq. (1) and Eq. (2)
amb	ambient
c	molar value
calc	calculated
cond	conductive
conv	convective
dG	dry gas
f	liquid surface temperature
G	gas or bulk gas temperature above the liquid surface
i	running number
j	upper limit
L	liquid
meas	measured
sat	saturation
v	liquid vapor

CRediT authorship contribution statement

Tibor Poós: Supervision, Resources, Project administration, Methodology, Investigation, Funding acquisition, Conceptualization. **Evelin Varju:** Writing – review & editing, Writing – original draft, Visualization, Validation, Software, Formal analysis, Data curation.

Declaration of competing interest

The authors declare that they have no known competing financial interests or personal relationships that could have appeared to influence the work reported in this paper.

Data availability

No data was used for the research described in the article.

Acknowledgements

This work was supported by the János Bolyai Research Scholarship of the Hungarian Academy of Sciences (BO/00059/23/6) and by the Hungarian Scientific Research Fund (NKFIH FK-142204). The second author was supported by the ÚNKP-23-5-BME-411 New National Excellence Program of the Ministry for Culture and Innovation from the source of the National Research, Development and Innovation Fund.

References

[1] E. Sartori, A critical review on equations employed for the calculation of the evaporation rate from free water surfaces, Sol. Energy 68 (2000) 77–89, https://doi.org/10.1016/S0038-092X(99)00054-7.
[2] M.M. Shah, Improved model for calculation of evaporation from water pools, Sci. Technol. Built Environ. 24 (2018) 1064–1074, https://doi.org/10.1080/23744731.2018.1483157.
[3] G.W. Himus, J.W. Hinchley, The effect of a current of air on the rate of evaporation of water below the boiling point, J. Soc. Chem. Ind. 43 (1924) 840–845, https://doi.org/10.1002/jctb.5000433402.
[4] M.T. Pauken, An experimental investigation of combined turbulent free and forced evaporation, Exp. Thermal Fluid Sci. 18 (1998) 334–340, https://doi.org/10.1016/S0894-1777(98)10038-9.
[5] M. Moghiman, A. Jodat, Effect of air velocity on water evaporation rate in indoor swimming pools, Iran. J. Mech. Eng. 8 (2007) 19–30.
[6] R.W. Powell, Evaporation of water from saturated surfaces I, Engineering 150 (1940) 238–239.
[7] A.F. Meyer, Evaporation from Lakes and Reservoirs, Minnesota Resources Commission, St. Paul, Minn, 1942.
[8] M.A. Kohler, T.J. Nordenson, W.E. Fox, Evaporation from Pans and Lakes, US Weather Bur. Res. Pap, 1955.
[9] W. McMillan, Heat dispersal-Lake Trawsfynydd cooling studies, Symp. Freshw. Biol. Electr. Power Gener. Part 1 (1) (1971) 41–79.
[10] M.S. Govind, Sodha, thermal model of solar swimming pools, Energy Convers. Manag. 23 (1983) 171–175, https://doi.org/10.1016/0196-8904(83)90060-2.
[11] E. Hahne, R. Kübler, Monitoring and simulation of the thermal performance of solar heated outdoor swimming pools, Sol. Energy 53 (1994) 9–19, https://doi.org/10.1016/S0038-092X(94)90598-3.
[12] C.C. Smith, G. Löf, R. Jones, Measurement and analysis of evaporation from an inactive outdoor swimming pool, Sol. Energy 53 (1994) 3–7, https://doi.org/10.1016/S0038-092X(94)90597-5.
[13] P. Ryan, J.D. Harleman, An Analytical and Experimental Study of Transient Cooling Pond Behavior, Ralph M Parsons Lab. Water Resour. Hydrodyn. Rep, 1973.
[14] V.V.N. Kishore, V. Joshi, A practical collector efficiency equation for nonconvecting solar ponds, Sol. Energy 33 (1984) 391–395, https://doi.org/10.1016/0038-092X(84)90190-7.

[15] D. Subhakar, S.S. Murthy, Saturated solar ponds: 1. Simulation procedure, Sol. Energy 50 (1993) 275–282, https://doi.org/10.1016/0038-092X(93)90021-F.
[16] C.O. Bennett, J.E. Myers, Momentum, Heat, and Mass Transfer, 2nd ed, McGraw-Hill, New York, 1974. http://trove.nla.gov.au/version/44867893 (accessed October 13, 2017).
[17] P.K. Raj, J.A. Morris, Source Characterization of Heavy Gas Dispersion Models for Reactive Chemicals, Technology and Management Systems Inc., Burlington MA, 1987.
[18] K.O. Braun, K.J. Caplan, Evaporation Rate of Volatile Liquids, Pace Laboratories, Minneapolis, 1992. https://ntrl.ntis.gov/NTRL/dashboard/searchResults/titleDetail/PB92232305.xhtml (accessed August 13, 2018).
[19] L. Olander, Equations and Formulas for Air and Air Contaminants - a Literature Review, Arbets Miljo Institute, National Institute of Occupational Health, Solna, Sweden, 1994.
[20] A.A. Hummel, K.O. Braun, M.C. Fehrenbacher, Evaporation of a liquid in a flowing airstream, Am. Ind. Hyg. Assoc. J. 57 (1996) 519–525, https://doi.org/10.1080/15428119691014729.
[21] US EPA, Risk Management Program Guidance for Offsite Consequences Analysis, United States Environmental Protection Agency, Washington D.C, 1999.
[22] Eastern Research Group, Preferred and Altenative Methods for Estimating Air Emissions from Paint and Ink Manufacturing Facilities, 2000.
[23] F. Heymes, L. Aprin, A. Bony, S. Forestier, S. Cirocchi, G. Dusserre, An experimental investigation of evaporation rates for different volatile organic compounds, Process. Saf. Prog. 32 (2013) 193–198, https://doi.org/10.1002/prs.11566.
[24] E. Varju, T. Poós, Atmospheric Evaporation of Open, Still Water Surface under Steady-State Conditions, Budapest University of Technology and Economics, 2023. https://repozitorium.omikk.bme.hu/handle/10890/41828.
[25] L. Tugyi, Z. Siménfalvi, G. Szepesi L, Experimental and theoretical investigation of acetone evaporation, Multidiszcip. Tudományok 11 (2021) 132–144, https://doi.org/10.35925/j.multi.2021.5.13.
[26] Acetone Solvent - 6 Common Acetone Uses (n.d.), https://ecolink.com/info/acetone-solvent-uses/ (accessed March 18, 2024).
[27] M. Weiner L, L. Kotkoskie A, Excipient Toxicity and Safety, CRC Press, 1999.
[28] MSHA - Safety Hazard Information - Special Hazards of Acetylene, n.d.), https://arlweb.msha.gov/alerts/hazardsofacetylene.htm (accessed August 12, 2018).
[29] Apollo application (n.d.), https://www.interconnect.hu/index2_hu.php (accessed March 13, 2023).
[30] W.L. McCabe, J.C. Smith, P. Harriott, Unit Operations in Chemical Engineering, 5th Revised edition edition, McGraw-Hill Inc., US, New York, 1993.
[31] N.H. Chen, D.F. Othmer, New generalized equation for gas diffusion coefficient, J. Chem. Eng. Data 7 (1962) 37–41, https://doi.org/10.1021/je60012a011.
[32] J.M. Bland, D.G. Altman, Statistical methods for assessing agreement between two methods of clinical measurement, Lancet Lond. Engl. 1 (1986) 307–310.